Construction of Acenaphthylenes via C–H Activation-Based Tandem Penta- and Hexaannulation Reactions

Jingsong You

jsyou@scu.edu.cn

Sichuan University https://orcid.org/0000-0002-0493-2388

Jian Li

Sichuan University

Tao Liu

Sichuan University

Junjie Liu

Sichuan University

Cheng Zhang

Sichuan University

Yudong Yang

Sichuan University https://orcid.org/0000-0002-7142-2249

Guangying Tan

Sichuan University

Article

Keywords:

Posted Date: June 27th, 2024

DOI: https://doi.org/10.21203/rs.3.rs-4598677/v1

Additional Declarations: There is **NO** Competing Interest.

Version of Record: A version of this preprint was published at Nature Communications on September 27th, 2024. See the published version at https://doi.org/10.1038/s41467-024-52652-4.

Abstract

Acenaphthylene-containing polycyclic aromatic hydrocarbons (AN-PAHs) are noteworthy structural motifs for organic functional materials due to their non-alternant electronic structure, which increases electron affinity. However, the synthesis of AN-PAHs has traditionally required multiple sequential synthetic steps, limiting structural diversity. Herein, we present a novel tandem C–H penta- and hexaannulation reaction of aryl alkyl ketone with acetylenedicarboxylate. This integrated approach enhances overall efficiency and selectivity, marking a significant advancement in AN-PAH synthesis. Mechanistic studies unveil an orchestrated extension of five- and six-membered rings through C–H activation-annulation and Diels–Alder reaction. Additionally, the tandem annulation reaction can be performed stepwise, further validating the proposed mechanism and increasing the structural diversity of AN-PAHs.

Introduction

Polycyclic aromatic hydrocarbons (PAHs) featuring non-hexagonal rings have attracted significant interest in the realm of organic optoelectronics[1-4]. Among these, acenaphthylene (AN)-containing PAHs stand out as exceptional structural units for organic functional materials, courtesy of their non-alternant electronic structure that enhances electron affinity (Fig. 1a)[5-12]. Consequently, the efficient synthesis of these compounds has garnered considerable attention. Traditional synthetic routes to AN-PAHs typically begin with the substitution, oxidation or annulation reactions of acenaphthene[13-16]. Nevertheless, these methods usually require multistep manipulation, and suffer from limitation of structural diversity. Recently, the advent of transition metal-catalyzed annulations has propelled significant advancements in the synthesis of AN-PAHs through catalytic strategies[17-20]. For instance, such PAHs could be obtained through palladium-catalyzed cyclopentaannulation reactions of halogenated naphthalenes with alkynes[21-23] or 2-halogenated arylboronic acids[24-26] (Fig. 1b). Despite significant progress, the development of a streamlined approach to access a variety of AN-PAHs, ideally utilizing abundant feedstocks, remains an appealing task in synthetic chemistry.

Aryl ketones are readily accessible chemicals and fundamental building blocks in organic synthesis. In recent years, transition metal-catalyzed *ortho*-C–H activation and functionalization of aryl ketones have been studied extensively [27-44]. Among these transformations, the direct C–H annulation reactions of aryl ketones with alkynes have emerged as a versatile strategy for the construction of π-conjugated molecules, as exemplified by the pioneering works of Glorius[27], Cheng[28], Wang[29], Maji[45], and our group[46-48]. Despite these advances, most studies have used aryl or alkyl alkynes as substrates for annulation reactions. The aryl or alkyl fragments are often difficult to transform or remove from the formed PAHs, limiting the practical utility of these reactions.

Dimethyl acetylenedicarboxylate (DMAD), an electron-deficient alkyne diester, is widely used in Michael reactions, cyclizations (Diels-Alder and 1,3-dipole) but rarely in transition metal-catalyzed C–H activation-

annulations[49]. Recently, we demonstrated its capability in C–H activation-annulation reaction with naphthalene ketones to generate aromatic polycarboxylic esters, establishing an efficient strategy for the synthesis of graphene-like molecules by utilizing the removability of ester groups as a key point[50]. Inspired by these studies, we envisaged that its annulation reaction with aryl ketones could rapidly access AN-containing PAHs. In the proposed reaction, a fulvene species, generated from the transition metal-catalyzed C–H activation-annulation of aryl ketone with alkyne, could be a key intermediate. The main challenge lies in effectively coupling the C–H activation-annulation with the Diels-Alder reaction. As proof of concept, we herein disclose an unprecedented tandem C–H penta- and hexaannulation reaction of aryl alkyl ketones with acetylenedicarboxylates, offering access to a diverse array of AN-PAHs in an atom- and step-economical manner (Fig. 1c). This reaction demonstrates high chemo- and regioselectivity, with the extension of five- and six-membered rings proceeding in an orchestrated pathway.

Results and Discussion

Optimization of the Reaction Conditions. At the onset of the optimization study, 1-(naphthalen-2-yl)ethan-1-one (**1a**) was chosen as model substrate to react with DMAD (**2a**). To our satisfaction, systematic evaluation of reaction parameters led to the highest yield of the desired product **3** at 62% under an optimized reaction conditions: **1a** (0.1 mmol, 1.0 equiv.), **2a** (0.4 mmol, 4.0 equiv.), $[Cp^*RhCl_2]_2$ (5 mol%), AgOTf (20 mol%), CuO (0.3 mmol, 3.0 equiv.), and 1-methylcyclohexane-1-carboxylic acid (1-MeCHA) (50 mol%) in DCE (2.0 mL) under a N_2 atmosphere at 150 ℃ for 16 h (Fig. 2a). The structure of **3** was confirmed by X-ray crystallography (Fig. 2a). Blank experiments revealed the indispensability of $[Cp^*RhCl_2]_2$, CuO, and 1-MeCHA for this transformation (Fig. 2b, entries 2–3). $[(p\text{-cymene})RuCl_2]_2$ showed negligible catalytic activity (Fig. 2b, entry 4). Replacing AgOTf with $AgSbF_6$ or $AgBF_4$ led to diminished yields of **3**, and the reaction ceased completely when AgTFA was used as an additive (Fig. 2b, entry 5). Other copper oxidants such as $Cu(OAc)_2$, Cu_2O, and $CuBr_2$ were proven less effective than CuO (Fig. 2b, entry 6). Moreover, this reaction exhibited robustness towards various organic acid additives, as replacing 1-MeCHA with PivOH, $MesCO_2H$ or $1\text{-}AdCO_2H$ (Fig. 2b, entries 7–8). Furthermore, the choice of solvent significantly influenced the transformation. Replacement of DCE with PhCl or toluene resulted in yields of **3** in 26% or 8% (Fig. 2b, entry 9). The reaction did not occur at all when using THF, DMF or MeCN as solvents (Fig. 2b, entry 10). Additionally, a reaction condition-based sensitivity screening indicated that this process was relatively robust in the face of small changes in concentration and temperature, high oxygen level, moisture, and scale-up (Fig. 2c, see Supporting Information for the details)[51].

Substrate Scope. With the optimized reaction conditions in hand, we embarked on a comprehensive exploration of the substrate scope using various aryl ketones **1**. As summarized in Fig. 3, 1-(naphthalen-2-yl)ethan-1-ones, equipped with electron donating groups such as methyl, methoxy, phenoxy, benzyloxy, pivaloyloxy, hydroxyl, 4-bromobutoxy, and even methylthio on the naphthyl ring, smoothly underwent this tandem annulation reaction, providing the corresponding AN-PAHs in moderate to good yields (Fig. 3, 3–11). The hydrolysis of compound **3** was achieved by refluxing it in a KOH solution composed of water

and THF, resulting in the corresponding tetraacid **3'** in a 96% yield. The versatility of the method was further demonstrated with the successful engagement of substrates featuring halogen substituents (fluoro, chloro, bromo) and electron withdrawing groups (ester and formyl), showing the potential for late-stage modification of the annulation products (Fig. 3, 12–16).

The applicability of the reaction extended to naphthalene ketones with aryl or heteroaryl substituents, affording the desired products in moderate yields (Fig. 3, 17–20). Encouragingly, even simple phenyl ketones, such as acetophenone (**1s**) and 1-(4-methoxyphenyl)ethan-1-one (**1t**), participated in the reaction to yield products **21** and **22**. The structure of **21** was confirmed by X-ray crystallography (Table S5). In addition, the protocol successfully accommodated larger π-conjugated ketones, including 1-(phenanthren-2-yl)ethan-1-one (**1u**), 1-(pyren-2-yl)ethan-1-one (**1v**), 1,1'-(pyrene-2,7-diyl)bis(ethan-1-one) (**1w**), 1-(anthracen-2-yl)ethan-1-one (**1x**), and 1-(chrysen-2-yl)ethan-1-one (**1y**), yielding the corresponding AN-PAHs in good yields (Fig. 3, 23–27). Moreover, other electron-deficient alkyne diesters (**2b**-**2c**) or diketone (**2d**) also participated in this reaction, delivering the corresponding products in moderate yields (Fig. 3, 28–30). Furthermore, for a comprehensive overview of the substrate scope, details on unsuccessful substrates are given in the Supporting Information (see Table S2 for the details).

To further demonstrate the versatility of this protocol, a bidirectional annulation reaction of 1,1'-(naphthalene-2,6-diyl)bis(ethan-1-one) (**1z**) with **2a** was conducted, affording a two acenaphthylene-containing PAH **32** in a synthetically useful yield (Fig. 4a). Subsequently, we conducted density functional theory (DFT) calculations to explore the photophysical and aromatic properties of compound **32**. Figure 4c illustrates that the lowest unoccupied molecular orbital (LUMO) of **32** is distributed across the entire molecule skeleton, while the highest occupied molecular orbital (HOMO) predominantly resides along the long axis of **32**. The LUMO and HOMO energy levels of **32** are − 3.47 and − 6.42 eV, respectively, demonstrating promise for semiconductor applications. The UV-vis and fluorescence spectra revealed maximum absorption and emission peaks of **32** at 430 nm and 543 nm (green fluorescence), respectively (Fig. 4d). To further investigate the stereo-electronic structure and aromaticity of **32**, we conducted two-dimensional nucleus-independent chemical shift (2D-NICS)[52] and anisotropy of the induced current density (ACID)[53] analysis (Fig. 4e and 4f). The results of these calculations indicate that the six-membered rings (rings 1, 2, 3 and 4) exhibit typical aromatic properties, as evidenced by negative 2D-NICS values (Fig. 4b and 4e) and a clockwise ring current along the perimeter of the chrysene core (Fig. 4f). In contrast, positive 2D-NICS values (Fig. 4e) and an anticlockwise direction of the ring current suggest the anti-aromaticity of the five-membered rings (rings 5 and 6) (Fig. 4b and 4f).

Mechanism Study. To gain some insight into the reaction mechanism, several control experiments were conducted. Initially, treatment of 1-(1-methylnaphthalen-2-yl)ethan-1-one (**1aa**) with **2a** under the standard reaction conditions afforded product **33** in 7% yield. In contrast, the reaction of **1ab** and **2a** produced only a byproduct **34** in 38% yield, arising from the trimerization of **2a**, with substrates **1ab** and **2a** being recovered in 92% and 28% yields, respectively (Fig. 5a). These outcomes suggested that the reaction might commence with the C3 − H activation and cyclopentaannulation of 1-(naphthalen-2-yl)ethan-1-one to form an intermediate with a five-membered ring. Indeed, a fulvene-containing

intermediate **35** was obtained in 44% yield from the reaction between 1-(naphthalen-2-yl)propan-1-one (**1ac**) and **2a**. Simultaneously, the acenaphthylene-containing product **36** was afforded in 17% yield, confirming the above conjecture (Fig. 5b). To clarify the subsequent cyclohexaannulation, compound **35** was subjected to further reaction with **2a** in the presence of AgOTf and CuO, excluding $[Cp^*RhCl_2]_2$, resulting in the desired product **36** in 42% yield (Fig. 5b). The structures of **33** and **36** were confirmed by X-ray crystallography (Table S6 and S7). These findings suggested that the hexaannulation might proceed through a Diels–Alder reaction, and the rhodium catalyst is likely not involved in this step. Subsequently, the chemical kinetics of the reaction of **1c** and **2a** were studied using in situ infrared (IR) measurements (Fig. 5c). Encouragingly, the absorption intensities of **1c**, **2a**, and **5** could be monitored by in situ IR measurements, tracked by change of the peaks at 1683, 1731, 1540 cm^{-1}, respectively (Fig. 5c, (i)). The kinetic profile showed that this annulation reaction proceeded relatively fast without a discernible induction period, with the majority of **5** formed within three hours (Fig. 5c, (ii-iii)).

Based on the above observations, we propose a mechanism of the reaction between **1a** and **2a**, involving C–H activation-annulation and Diels–Alder reaction (Fig. 6a). The reaction initiates with a ketone-directed C3–H activation of **1a** with Cp^*RhX_2 (X = OTf or RCO_2) to form a five-membered cyclorhodium intermediate **I**. Subsequently, intermediate **I** chelates with **2a**, leading to the formation of intermediate **II**. Alkyne insertion and subsequent intramolecular electrophilic attack of the carbonyl unit generate intermediate **IV**. Transmetalation of intermediate **IV** with copper carboxylate salt yields intermediate **VI** and Cp^*RhX_2 through a transitional intermediate **V**. *beta*-Hydrogen elimination of intermediate **VI** produces intermediate **VII**. A Diels–Alder reaction of intermediate **VII** with **2a** delivers intermediate **VIII**, corroborated by a high-resolution mass spectrometry (HRMS) determination (Fig. S5, m/z calcd: 459.1050, found: 459.1046). Finally, intermediate **VIII** undergoes further oxidative aromatization in the presence of copper or silver salts to produce the desired product **3**.

After investigating the reaction mechanism, we speculated that the tandem penta- and hexaannulation reaction could be achieved stepwise by adjusting the reaction conditions. To test this hypothesis, we conducted stepwise annulation reactions of acetophenone (**1s**) with two electronically differentiated alkynes (Fig. 6b). Under slightly modified Rh-catalyzed conditions, acetophenone (**1s**) reacted with various diphenyl alkynes, affording a series of 1-methylene-2,3-diaryl-1*H*-indenes (37–43) in good yields. These intermediates then underwent a Diels–Alder reaction with DMAD (**2a**), producing the desired AN-PAHs (44–50). The structure of **44** was confirmed by X-ray crystallography (Table S8). These results further verified the proposed reaction mechanism and expanded the structural diversity of the AN-PAHs. To demonstrate the practicality of this reaction, several derivatizations of product **44** were conducted (Fig. 6c). Hydrolysis of **44** yielded diacid **51**, which further underwent a condensation reaction to produce imide product **52** or a decarboxylation reaction to generate product **53**. Finally, treatment of **53** with $FeCl_3$ and DDQ in dichloromethane for 2 h delivered product **54** in a 68% yield.

Conclusion

In summary, we have introduced a novel tandem C–H annulation reaction of aryl alkyl ketones with acetylenedicarboxylates, offering a straightforward and rapid method to access a series of AN-PAHs from abundant feedstocks in a single step. This reaction demonstrates high chemo- and regioselectivity, a broad substrate scope, and excellent functional group tolerance. Mechanism studies has elucidated a comprehensive pathway involving Rh-catalyzed C–H cyclopentaannulation, followed by a Diels–Alder reaction. Additionally, stepwise annulation reactions of acetophenone with two electronically differentiated alkynes verified the proposed mechanism and expanded the structural diversity of AN-PAHs. We anticipate that this work will captivate the synthetic community, offering a valuable toolkit for materials chemists to explore novel acenaphthylene-based organic functional materials.

Methods

General procedure for tandem C – H penta- and hexaannulation reactions

A 25 mL Schlenk tube with a magnetic stir bar was charged with $[Cp^*RhCl_2]_2$ (3.1 mg, 5 mol%), AgOTf (5.1 mg, 20 mmol%), CuO (24.0 mg, 0.3 mmol, 3.0 equiv.), 1-MeCHA (7.1 mg, 0.05 mmol, 0.5 equiv.), naphthalene ketone **1** (0.1 mmol, 1.0 equiv.) and alkyne **2** (0.4 mmol, 4.0 equiv.) in DCE (2.0 mL) under N_2 atmosphere. The resulting mixture was stirred at 150 °C for 16 h. The resulting solution was cooled to ambient temperature, diluted with 10 mL of CH_2Cl_2, filtered through a celite pad, and washed three times with 10 mL of CH_2Cl_2. The obtained organic extracts were evaporated under reduced pressure and the residue was absorbed into small amounts of silica gel. Purification was performed by column chromatography on silica gel to provide the desired product.

Declarations

Acknowledgements

This work was supported by National Key R&D Program of China (No. 2021YFA1500100, Y.Y.), National Natural Science Foundation of China (No. 22031007, J.Y., 22171188, Y.Y.), and the Fundamental Research Funds for the Central Universities (YJ202340, G.T., 2023SCUH0080, Y.Y.). We also thank the support from the Analytical and Testing Center of Sichuan University, and Dr. J. Li and Dr. C. Wang from Comprehensive Training Platform Specialized Laboratory, College of Chemistry, Sichuan University.

Author contributions

J.L., T.L., Y.Y. and C.Z. performed the experiments and analyzed the data. J.L. performed DFT calculations. G.T. and J.Y. designed and directed the project. J.L., G.T. and J.Y. wrote the manuscript. All authors contributed to discussions.

Additional information

Accession codes: The X-ray crystallographic coordinates for structures reported in this article have been deposited at the Cambridge Crystallographic Data Centre (CCDC) under deposition number CCDC 2326151 (**3**), 2326160 (**21**), 2326156 (**33**), 2326157 (**36**), and 2360166 (**44**). These data can be obtained free of charge from The Cambridge Crystallographic Data Centre via www.ccdc.cam.ac.uk/data_request/cif.

Data availability

The data that support the findings of this study are available within the article and its Supplementary Information. Extra data are available from the corresponding authors upon reasonable request.

Competing interests

The authors declare no competing interests.

References

1. Rickhaus M, Mayor M, Juríčeka M (2017) Chirality in curved polyaromatic systems. Chem Soc Rev 46:1643–1660
2. Pun SH, Miao Q (2018) Toward negatively curved carbons. Acc Chem Res 51:1630–1642
3. Chaolumen, Stepek IA, Yamada KE, Ito H, Itami K (2021) Construction of heptagon-containing molecular nanocarbons. Angew Chem Int Ed 60:23508–23532
4. Fei Y, Liu J (2022) Synthesis of defective nanographenes containing joined pentagons and heptagons. Adv Sci 9:2201000
5. Stuparu MC (2021) Corannulene: a curved polyarene building block for the construction of functional materials. Acc Chem Res 54:2858–2870
6. Liu Y-H, Perepichka DF (2021) Acenaphthylene as a building block for π-electron functional materials. J Mater Chem C 9:12448–12461
7. Ma L, Han Y, Shi Q, Huang H (2023) The design, synthesis and application of rubicene based polycyclic aromatic hydrocarbons (PAHs). J Mater Chem C 11:16429–16438
8. Jellison JL, Lee C-H, Zhu X, Wood JD, Plunkett K (2012) N. Electron acceptors based on an all-carbon donor-acceptor Copolymer. Angew Chem Int Ed 51:12321–12324
9. Sun X, Wu F, Zhong C, Zhu L, Li Z (2019) A structure-property study of fluoranthene-cored hole-transporting materials enables 19.3% efficiency in dopant-free perovskite solar cells. Chem Sci 10:6899–6907
10. Liu H, Fu Y, Tang B, Zhao Z (2022) All-fluorescence white organic light-emitting diodes with record-beating power efficiencies over 130 lmW^{-1} and small roll-offs. Nat Commun 13:5154
11. Kumar R, Chmielewski PJ, Lis T, Volkmer D, Stępień M (2022) Tridecacyclene tetraimide: an easily reduced cyclooctatetraene derivative. Angew Chem Int Ed 61:e202207486

12. Wu Z et al (2023) An in-situ cyanidation strategy to access tetracyanodiacenaphthoanthracene diimides with high electron mobilities exceeding 10 $cm^2V^{-1}s^{-1}$. Angew Chem Int Ed 62:e202307695
13. Amick AW, Scott LT (2007) Trisannulated benzene derivatives by acid catalyzed aldol cyclotrimerizations of cyclic ketones. Methodology development and mechanistic insight. J Org Chem 72:3412–3418
14. Li H et al (2013) Tetraazabenzodifluoranthene diimides: building blocks for solution-processable n-type organic semiconductors. Angew Chem Int Ed 52:5513–5517
15. Zhylitskaya H, Cybińska J, Chmielewski P, Lis T, Stępień M (2016) Bandgap engineering in π–Extended pyrroles. A modular approach to electron-deficient chromophores with multi-redox activity. J Am Chem Soc 138:11390–11398
16. Borstelmann J, Bergner J, Rominger F, Kivala M (2023) A negatively curved π-expanded pyracylene comprising a tropylium cation. Angew Chem Int Ed 62:e202312740
17. Alberico D, Scott ME, Lautens M (2007) Aryl – aryl bond formation by transition-metal-catalyzed direct arylation. Chem Rev 107:174–238
18. Jin T, Zhao J, Asao N, Yamamoto Y (2014) Metal-catalyzed annulation reactions for π-conjugated polycycles. Chem Eur J 20:3554–3576
19. Hagui W, Doucet H, Soulé J-F (2019) Application of palladium-catalyzed C(sp^2) – H bond arylation to the synthesis of polycyclic (hetero)aromatics. *Chem* 5, 2006 – 2078
20. Jolly A, Miao D, Daigle M, Morin J-F (2020) Emerging bottom-up strategies for the synthesis of graphene nanoribbons and related structures. Angew Chem Int Ed 59:4624–4633
21. Bheemireddy SR, Hautzinger MP, Li T, Lee B, Plunkett KN (2017) Conjugated ladder polymers by a cyclopentannulation polymerization. J Am Chem Soc 139:5801–5807
22. Qin L et al (2023) Diazulenorubicene as a non-benzenoid isomer of *peri*-tetracene with two sets of 5/7/5 membered rings showing good semiconducting properties. Angew Chem Int Ed 62:e202304632
23. Liu B et al (2023) Bespoke tailoring of graphenoid sheets: a rippled molecular carbon comprising cyclically fused nonbenzenoid rings. J Am Chem Soc 145:28137–28145
24. Jackson EA, Steinberg BD, Bancu M, Wakamiya A, Scott LT (2007) Pentaindenocorannulene and tetraindenocorannulene: new aromatic hydrocarbon π systems with curvatures surpassing that of C_{60}. *J. Am. Chem. Soc.* 129, 484 – 485
25. Seifert S, Schmidt D, Shoyama K, Würthner F (2017) Base-selective five- versus six-membered ring annulation in palladium-catalyzed C – C coupling cascade reactions: new access to electron-poor polycyclic aromatic dicarboximides. Angew Chem Int Ed 56:7595–7600
26. Labella J et al (2023) Naphthalimide-fused subphthalocyanines: electron-deficient materials prepared by cascade annulation. ACS Mater Lett 5:543–548
27. Patureau FW, Besset T, Kuhl N, Glorius F (2011) Diverse strategies toward indenol and fulvene derivatives: Rh-catalyzed C – H activation of aryl ketones followed by coupling with internal alkynes.

J Am Chem Soc 133:2154–2156

28. Muralirajan K, Parthasarathy K, Cheng C-H (2011) Regioselective synthesis of indenols by rhodium-catalyzed C – H activation and carbocyclization of aryl ketones and alkynes. Angew Chem Int Ed 50:4169–4172
29. Tan X et al (2012) Rhodium-catalyzed cascade oxidative annulation leading to substituted naphtho[1,8-*bc*]pyrans by sequential cleavage of C(sp^2) – H/C(sp^3) – H and C(sp^2) – H/O – H bonds. J Am Chem Soc 134:16163–16166
30. Zheng Q-Z, Jiao N (2014) Transition-metal-catalyzed ketone-directed *ortho*-C – H functionalization reactions. Tetrahedron Lett 55:1121–1126
31. Huang Z, Lim HN, Mo F, Young MC, Dong G (2015) Transition metal-catalyzed ketone-directed or mediated C – H functionalization. Chem Soc Rev 44:7764–7786
32. Sambiagio C et al (2018) A comprehensive overview of directing groups applied in metal-catalysed C–H functionalisation chemistry. Chem Soc Rev 47:6603–6743
33. Yang K, Song M, Liu H, Ge H (2020) Palladium-catalyzed direct asymmetric C–H bond functionalization enabled by the directing group strategy. Chem Sci 11:12616–12632
34. Mandal R, Garai B, Sundararaju B (2022) Weak-coordination in C – H bond functionalizations catalyzed by 3d metals. ACS Catal 12:3452–3506
35. Kim J, Chang S (2014) Iridium-catalyzed direct C – H amidation with weakly coordinating carbonyl directing groups under mild conditions. Angew Chem Int Ed 53:2203–2207
36. Raghuvanshi K, Zell D, Rauch K, Ackermann L (2016) Ketone-assisted ruthenium(II)-catalyzed C – H imidation: access to primary aminoketones by weak coordination. ACS Catal 6:3172–3175
37. Yang Y, Gao P, Zhao Y, Shi Z (2017) Regiocontrolled direct C – H arylation of indoles at the C4 and C5 positions. Angew Chem Int Ed 56:3966–3971
38. Kimura N, Kochi T, Kakiuchi F (2017) Iron-catalyzed regioselective anti-markovnikov addition of C – H bonds in aromatic ketones to alkenes. J Am Chem Soc 139:14849–14852
39. Tan G, You Q, You J (2018) Iridium-catalyzed oxidative heteroarylation of arenes and alkenes: overcoming the restriction to specific substrates. ACS Catal 8:8709–8714
40. Hu Y, Zhou B, Chen H, Wang C (2018) Manganese-catalyzed redox-neutral C – H olefination of ketones with unactivated alkenes. Angew Chem Int Ed 57:12071–12075
41. Chen S et al (2019) C2/C4 Regioselective heteroarylation of indoles by tuning C – H metalation modes. ACS Catal 9:6372–6379
42. Tan X et al (2021) Rhoda-electrocatalyzed bimetallic C – H oxygenation by weak *O*-coordination. Angew Chem Int Ed 60:13264–13270
43. Song S, Lai Y, Tuo Z, Zhong J, Zhou W (2023) Regio- and chemoselective formal (4 + 1) carbocyclization of chalcones with internal alkynes *via* rhodium(III) catalysis. Angew Chem Int Ed 62:e202305983

44. Cao Y-X, Wodrich MD, Cramer N (2023) Nickel-catalyzed direct stereoselective α-allylation of ketones with non-conjugated dienes. Nat Commun 14:7640
45. Sk MR, Bhattacharyya A, Saha S, Brahma A, Maji MS (2023) Annulative π-extension by rhodium(III)-catalyzed ketone-directed C – H activation: rapid access to pyrenes and related polycyclic aromatic hydrocarbons (PAHs). Angew Chem Int Ed 62:e202305258
46. Liu X, Li G, Song F, You J (2014) Unexpected regioselective carbon-hydrogen bond activation/cyclization of indolyl aldehydes or ketones with alkynes to benzo-fused oxindoles. Nat Commun 5:5030
47. Yin J, You J (2019) Concise synthesis of polysubstituted carbohelicenes by a C – H activation/radical reaction/C – H activation Sequence. Angew Chem Int Ed 58:302–306
48. Yin J et al (2019) Acyl radical to rhodacycle addition and cyclization relay to access butterfly flavylium fluorophores. Nat Commun 10:5664
49. Neochoritis CG, Zarganes-Tzitzikas T (2014) & Stephanidou- Stephanatou, J. Dimethy acetylenedicarboxylate: a versatile tool in organic synthesis. *Synthesis* 46, 0537 – 0585
50. Yin J et al (2023) Programmable zigzag π-extension toward graphene-like molecules by the stacking of naphthalene blocks. Nat Synth 2:838–847
51. Pitzer L, Sch-fers F, Glorius F (2019) Rapid assessment of the reaction-condition-based sensitivity of chemical transformations. Angew Chem Int Ed 58:8572–8576
52. Lu T, Chen F (2012) Multiwfn: a multifunctional wavefunction analyzer. *J. Comput. Chem.* 33, 580 – 592
53. Geuenich D, Hess K, Köhler F, Herges R (2005) Anisotropy of the induced current density (ACID), a general method to quantify and visualize electronic delocalization. Chem Rev 105:3758–3772

Figures

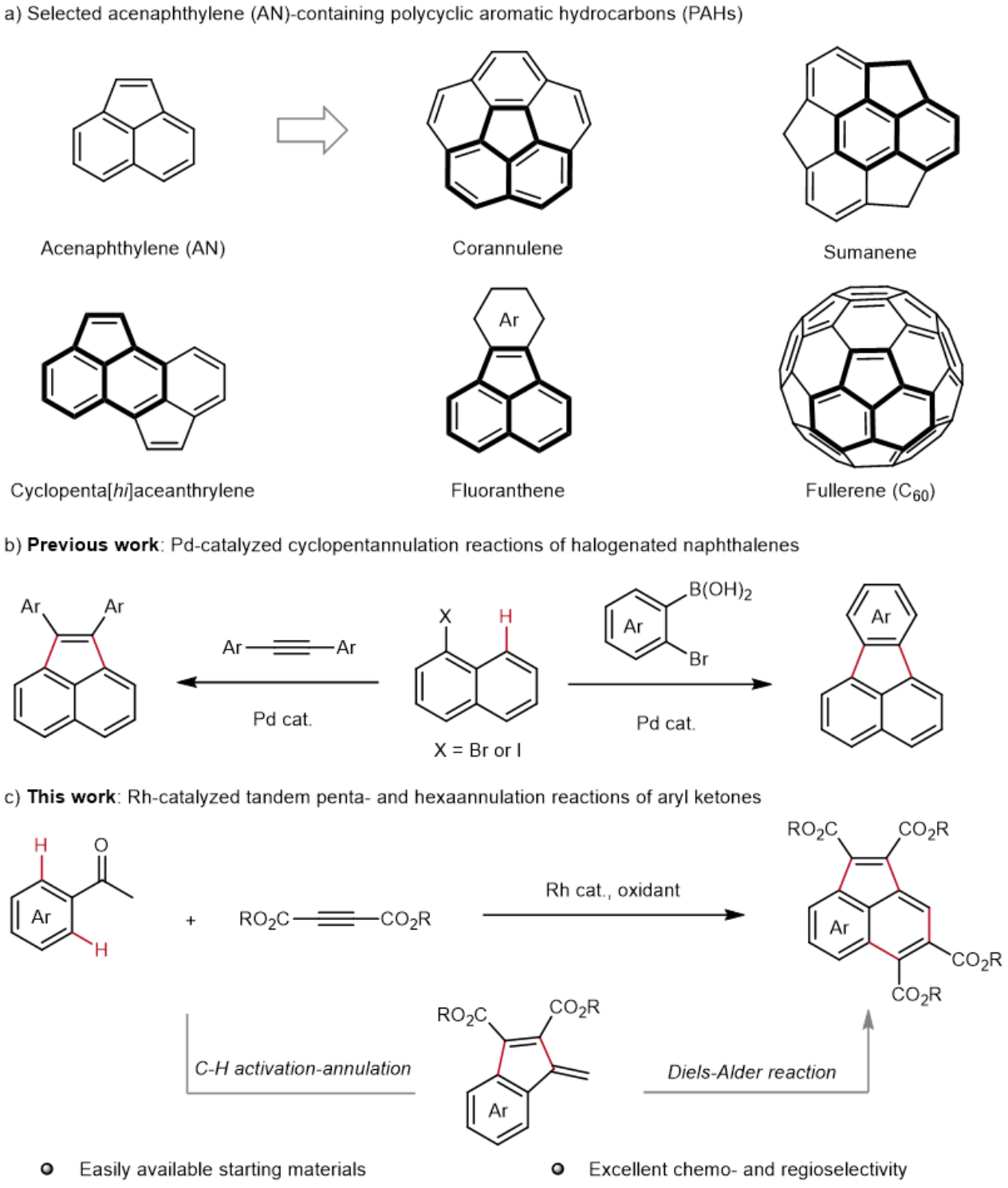

Figure 1

Acenaphthylene (AN)-containing polycyclic aromatic hydrocarbons (PAHs) and their synthetic strategies. a) Selected AN-containing PAHs. b) Previous work: Pd-catalyzed cyclopentannulation reactions of halogenated naphthalenes. c) This work: Rh-catalyzed tandem penta- and hexaannulation reactions of aryl ketones.

a) Standard reaction conditions

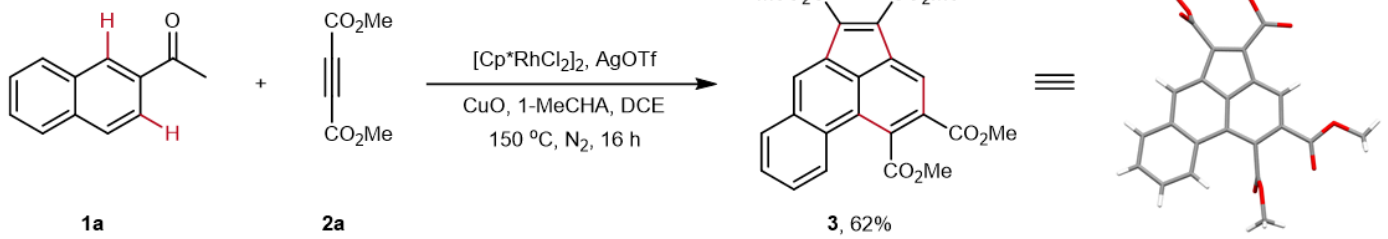

1a **2a** **3**, 62%

b) Impact of other reaction parameters

Entry	Variation from the *'standard conditions'*	Yield [%]
1	None	62
2	Without $[Cp^*RhCl_2]_2$	N.D.
3	Without CuO or 1-MeCHA	6, trace
4	$[(p\text{-cymene})RuCl_2]_2$ instead of $[Cp^*RhCl_2]_2$	trace
5	$AgSbF_6$, $AgBF_4$ or AgTFA instead of AgOTf	44, 37, N.D.
6	$Cu(OAc)_2$, Cu_2O or $CuBr_2$ instead of CuO	56, 51, N.R.
7	PivOH or CH_3CO_2H instead of 1-MeCHA	55, 39
8	$MesCO_2H$ or $1\text{-}AdCO_2H$ instead of 1-MeCHA	50, 54
9	PhCl or PhMe instead of DCE	26, 8
10	THF, DMF or MeCN instead of DCE	N.D.

c) Assessment of condition-based sensitivity

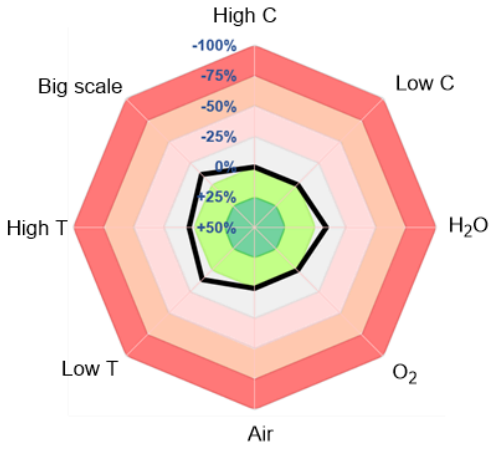

Figure 2

Optimization of the reaction conditions. a) Standard reaction conditions: **1a** (0.1 mmol, 1.0 equiv.), **2a** (0.4 mmol, 4.0 equiv.), $[Cp^*RhCl_2]_2$ (5 mol%), AgOTf (20 mol%), CuO (0.3 mmol, 3.0 equiv.), and 1-MeCHA (50 mol%) in DCE (2.0 mL) under N_2 atmosphere at 150 °C for 16 h. b) Impact of other reaction parameters. Isolated yields are given. c) Reaction condition-based sensitivity screening. 1-MeCHA: 1-methylcyclohexane-1-carboxylic acid.

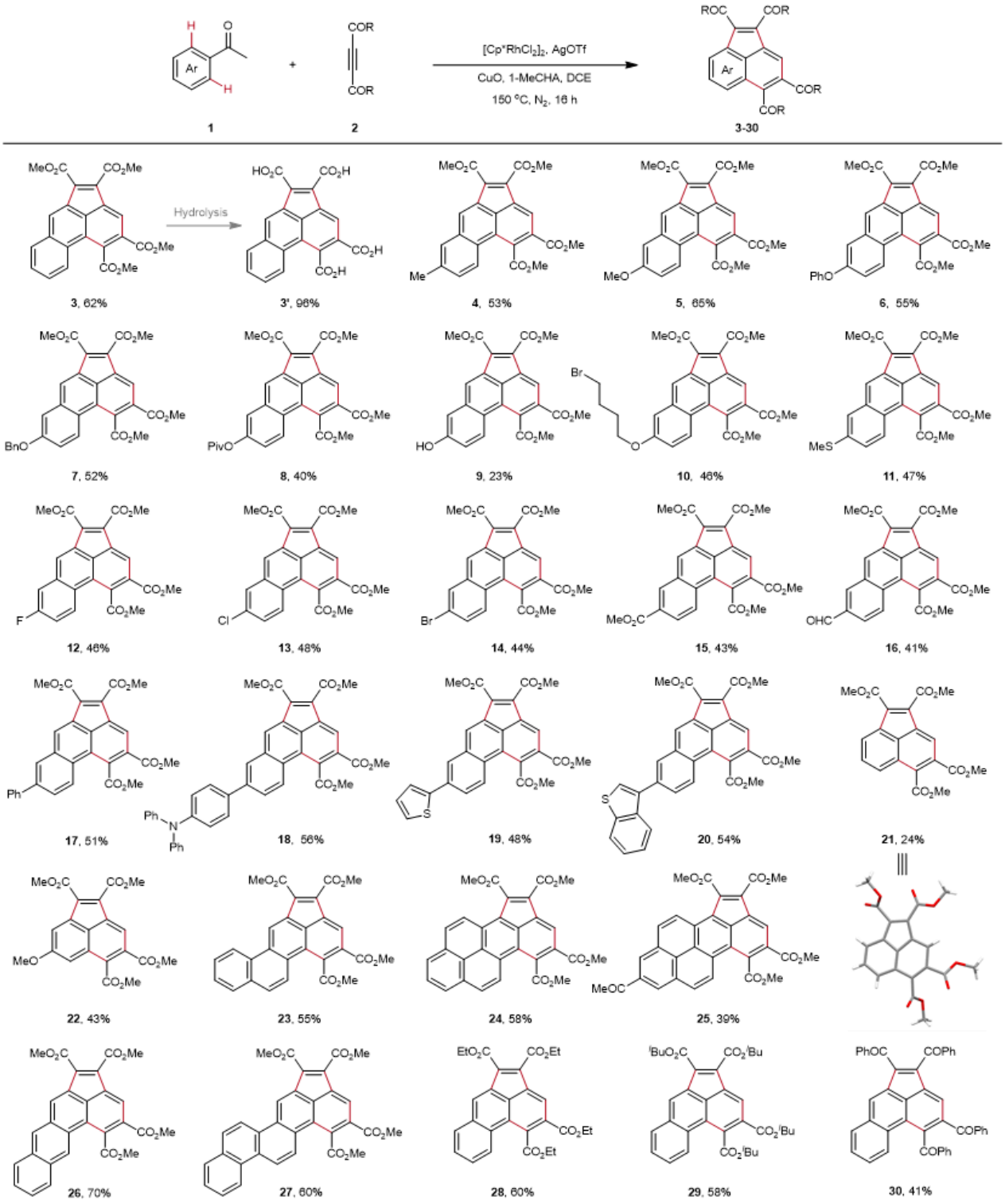

Figure 3

Scope of the reaction. Reactions run with **1** (0.1 mmol, 1.0 equiv.), **2** (0.4 mmol, 4.0 equiv.), $[Cp^*RhCl_2]_2$ (5 mol%), AgOTf (20 mol%), CuO (0.3 mmol, 3.0 equiv.), and 1-MeCHA (50 mol%) in DCE (2.0 mL) under N_2 atmosphere at 150 °C for 16 h. Reaction conditions of the hydrolysis: **3** (0.1 mmol, 1.0 equiv.) and KOH (2.0 mmol, 20.0 equiv.) in THF/H_2O (2.0 mL, 1:1, v/v) under N_2 atmosphere at 100 °C for 24 h.

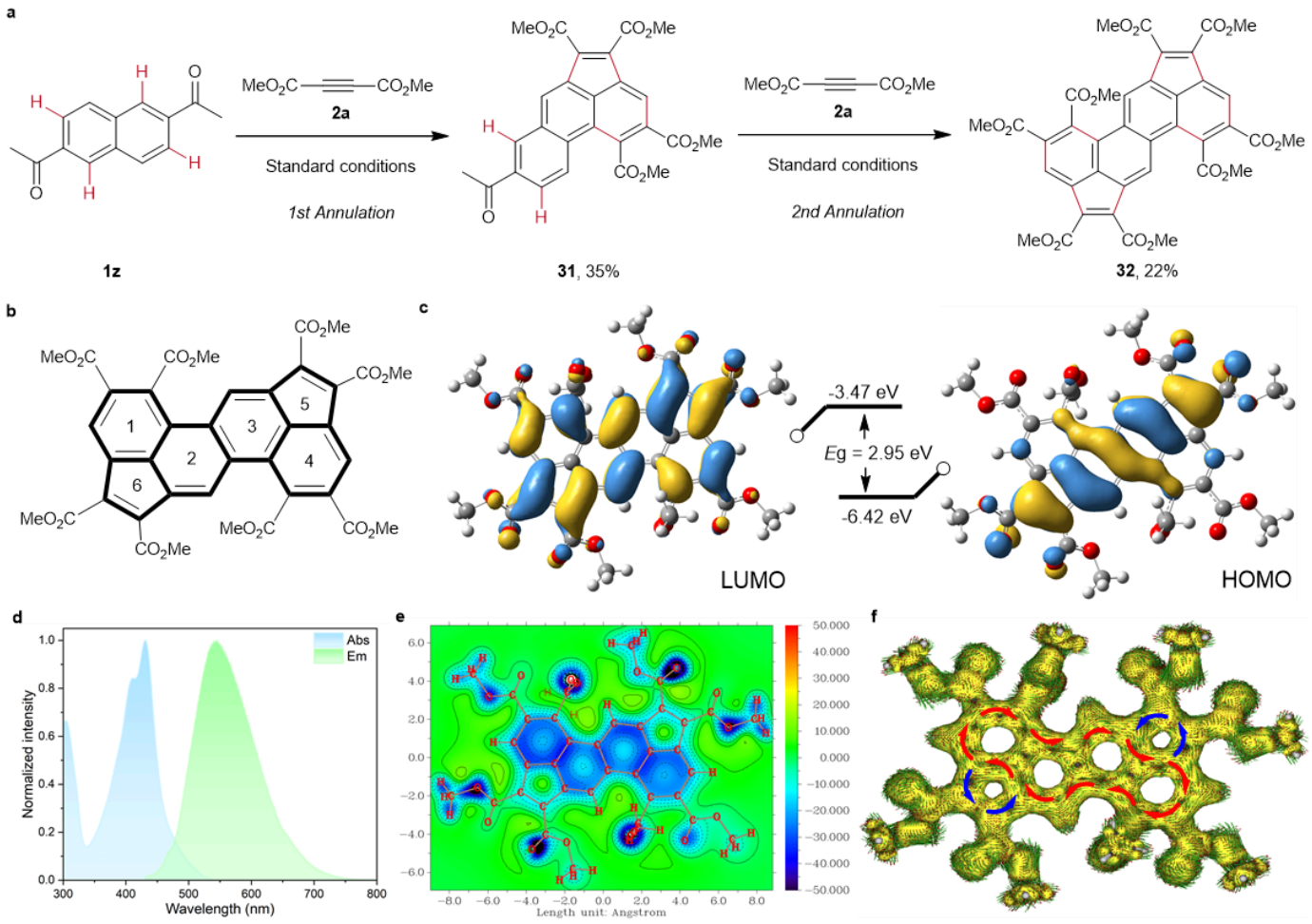

Figure 4

Bidirectional annulation reaction. a) Bidirectional annulation reaction of **1z** with **2a**. Reaction conditions: **1z** or **31** (0.1 mmol, 1.0 equiv.), **2a** (0.4 mmol, 4.0 equiv.), $[Cp^*RhCl_2]_2$ (5 mol%), AgOTf (20 mol%), CuO (0.3 mmol, 3.0 equiv.), and 1-MeCHA (50 mol%) in DCE (2.0 mL) under N_2 atmosphere at 150 °C for 16 h. b) The structure of **32**. c) The optimized molecular geometry and molecular orbitals (HOMO and LUMO) of **32**, calculated at the B3LYP/6-31G(d) level of theory. d) The absorption and emission spectra of **32** in dichloromethane (1×10^{-5} mol/L). e) The two-dimensional nucleus-independent chemical shift (2D-NICS) calculations of **32**, calculated at the B3LYP/6-31G(d) level of theory. f) The anisotropy of the induced current density (ACID) plots of **32**, calculated at the B3LYP/6-31G(d) level of theory. The red and blue arrows indicate the clockwise and anticlockwise ring currents, respectively.

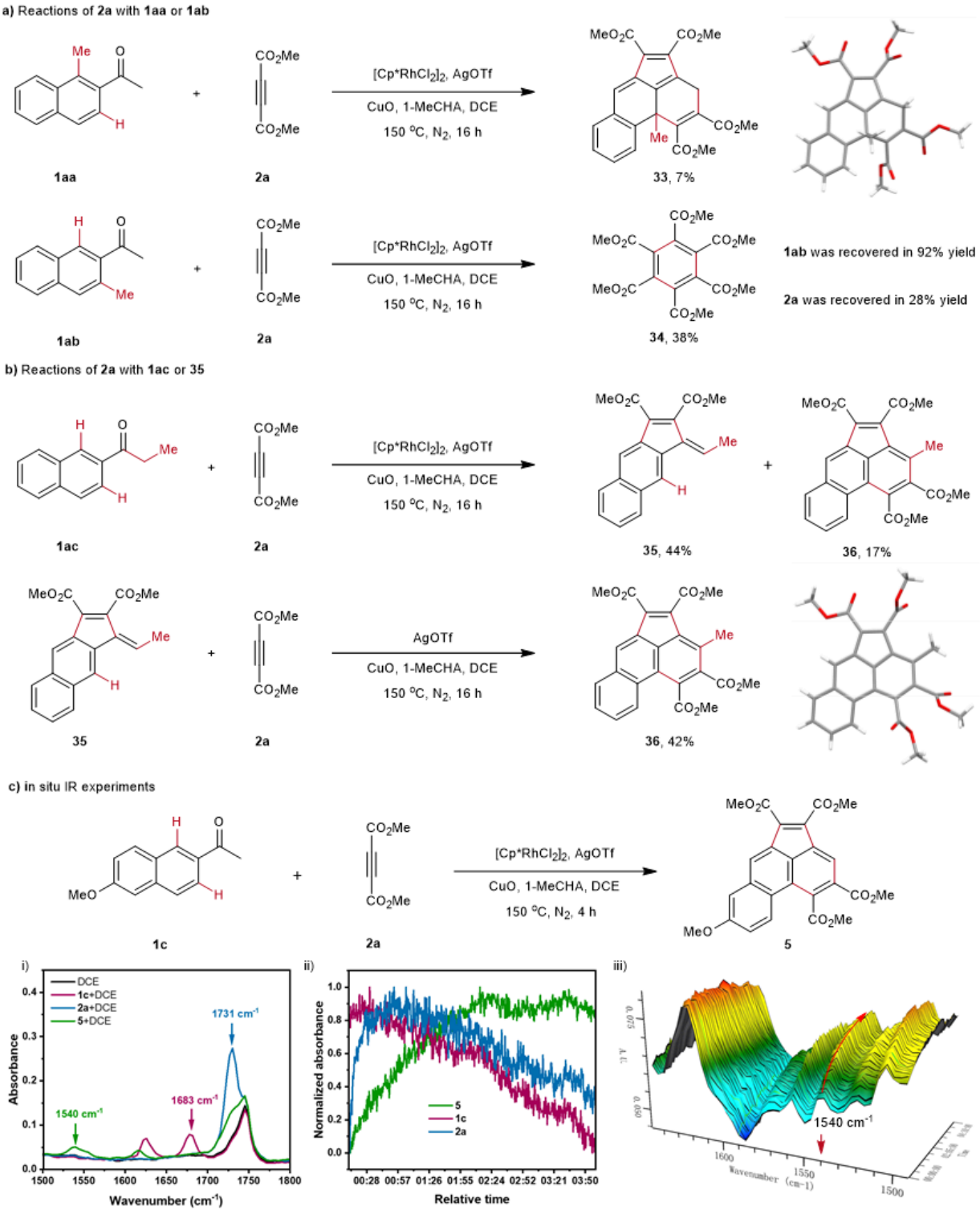

Figure 5

Mechanism study. a) Reactions of **1aa** or **1ab** with **2a** were performed under standard reaction conditions. b) Reaction of **1ac** with **2a** was performed under standard reaction conditions. Reaction of **35** with **2a** was performed without the addition of $[Cp^*RhCl_2]_2$. c) in situ IR experiments of **1c** and **2a**.

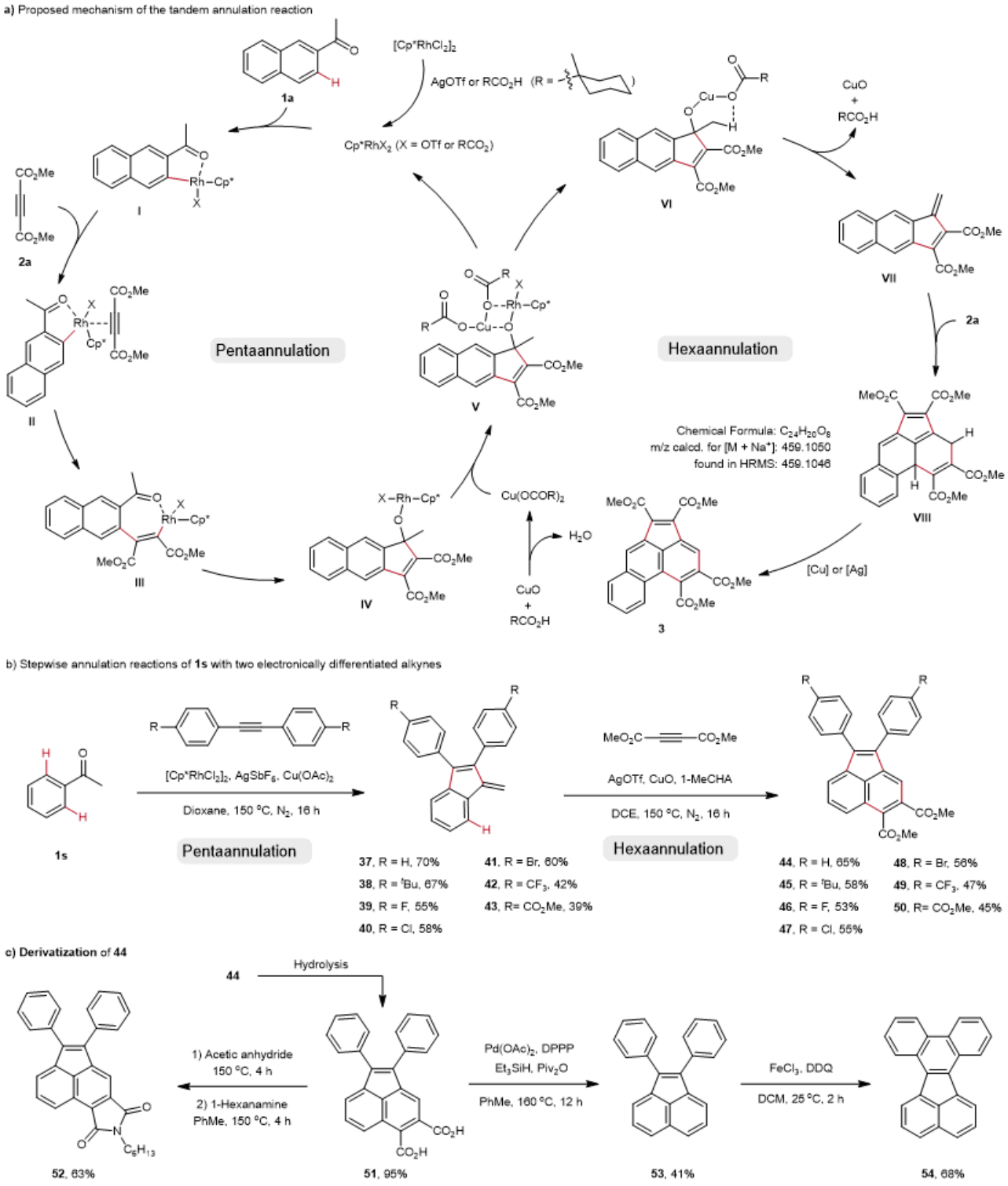

Figure 6

Proposed mechanism and stepwise annulation reactions. a) Proposed mechanism of the tandem annulation reaction. b) Stepwise annulation reactions of **1s** with two electronically differentiated alkynes (see part VIII of Supporting Information for the details). c) Derivatization of **44** (see part IX of Supporting Information for the details).

Supplementary Files

This is a list of supplementary files associated with this preprint. Click to download.

- SupportingInformation.pdf
- checkcif21.pdf
- checkcif3.pdf
- checkcif33.pdf
- checkcif36.pdf
- checkcif44.pdf
- cif21.cif
- cif3.cif
- cif33.cif
- cif36.cif
- cif44.cif